Forschungsschwerpunkt S92

Industrial Geometry

http://www.ig.jku.at

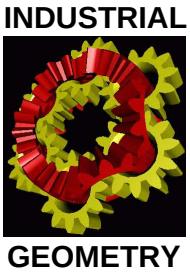

FSP Report No. 52

Segmentation of Biologic Image Data with A-Priori Knowledge

Matthias Fuchs and Otmar Scherzer

May 2007

FWF
Der Wissenschaftsfonds.

EVOLUTIONARY METHODS FOR DESIGN, OPTIMIZATION AND CONTROL
P. Neittaanmäki, J. Périaux and T. Tuovinen (Eds.)

SEGMENTATION OF BIOLOGIC IMAGE DATA WITH A-PRIORI KNOWLEDGE

Matthias Fuchs*

Infmath Imaging
University of Innsbruck
Technikerstr. 21a/2, 6020 Innsbruck, Austria
Email: matz.fuchs@uibk.ac.at
Web page: http://infmath.uibk.ac.at

Otmar Scherzer

Infmath Imaging
University of Innsbruck
Technikerstr. 21a/2, 6020 Innsbruck, Austria
Email: otmar.scherzer@uibk.ac.at
Web page: http://infmath.uibk.ac.at

Abstract. This work is concerned with the detection of geometries in 2D image data using statistical a-priori knowledge. We consider a Riemannian manifold of parametric shapes and a set of known training shapes in this metric space. From this data we compute a mean shape and the principal directions of the variances on the manifold. We use these results to regularize an edge-based segmentation functional and propose a simple Monte Carlo optimization technique which adapts itself to the statistical data. This technique is applied to the automatic detection of cells in biologic image data.

Key words: statistical shape analysis, variational methods, Monte Carlo optimization, image segmentation, shape recognition.

1 INTRODUCTION

The idea of deriving statistical knowledge from training data and deploying this information for detecting objects in image data has been considered in [1, 2, 3, 4, 5]. In these works the authors use either level set and or parametric representations of shapes and combine their statistics with various segmentation techniques such as geodesic active contours [6] and Mumford-Shah segmentation [7]. We are concerned with the extension of this idea to more general shape spaces. This leads to the statistical analysis on Riemannian manifolds and the derivation of statistically motivated segmentation techniques. We finally present an example which illustrates that the knowledge obtained from training data not only defines a suitable regularization term for the segmentation energy but can also be intelligently incorporated in algorithms used to minimize the regularization functional.

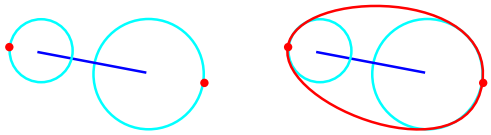

Figure 1: An element of the shape space M. The shape parameter $p \in M$ (dark blue skeleton and light blue atoms) is mapped to the shape $\psi(p)$ (red curve).

2 SHAPE MODEL

In this work the term *shape space* refers to a finite-dimensional parameter manifold M. Each *shape parameter* $p \in M$ defines the *shape* $\psi(p)$, which is a piecewise smooth curve without selfintersections.

The actual shape model we consider in applications is based on the medial axis representation and was developed in [8]. There the medial axis transform of shapes is parameterized instead of the actual boundary curve. In the special application presented in this paper we consider the shape space $M = \mathbb{R}^2 \times \mathbb{R}_+^2 \times (S^1 \times \mathbb{R}_+)$. A shape parameter $p \in M$ consists of a position, two positive radii and a vector (represented in polar coordinates). This data is mapped to the dark blue *skeleton* of the shape and the light blue *atoms* in Figure 1 on the left. The corresponding shape $\psi(p)$ is the red outline on right which interpolates the red points on the atoms. The skeleton can be interpreted as an approximation of the medial axis of the red shape. The atoms are the maximal circles inside the shape, centered at the vertices of the skeleton. This concept can be extended to more complex skeletons and a larger number of atoms.

Obviously M is the direct product of Riemannian manifolds. On $\mathbb{R}^2$ we assume the Euclidean metric, on S^1 the metric induced by the embedding of S^1 into $\mathbb{R}^2$ and on $\mathbb{R}_+$ the unique (up to scalar multiplication) metric on $\mathbb{R}_+$ which is invariant with respect to multiplication. From the metrics on each of its factors we derive the canonical product metric on M and denote it as $\langle \cdot, \cdot \rangle$. That is, the inner product of two tangent vectors $V, W \in T_pM$, $p \in M$, is given by $\langle V, W \rangle_p$.

For $p \in M$, this metric defines a chart, which maps a neighborhood $p \in \mathcal{V} \subseteq M$ to the tangent space T_pM: For $q \in \mathcal{V}$ let $V \in T_pM$ be such, that the geodesic γ defined by $\gamma(0) = p$ and $\dot{\gamma}(0) = V$ satisfies $\gamma(1) = q$. We call V the *logarithm of q in p*, denoted as $\mathrm{Log}_p(q) = V$. The inverse of Log_p is called the *exponential map in p*, denoted as Exp_p. For more details we refer e.g. to [9].

3 SHAPE STATISTICS

This section is devoted to the statistical analysis of data $p_1, \ldots, p_S$ on a shape manifold M. The basic idea of this analysis goes back to the *Principal Geodesic Analysis* (PGA) on manifolds proposed in [10]. This work generalizes the idea of the Principal Component Analysis (PCA) on vector spaces. The PCA of a given set of data points in a vector space V is an orthonormal basis of V such that the first basis vector points into the direction of the largest variance of the data, the second one into the direction of the second-largest variance and so on. Thus, the PCA can also be interpreted as sequence of orthogonal linear subspaces $V_n \subseteq V$ given by the linear hull of the n-th basis vector. On manifolds the concept of linear subspaces is replaced by *geodesic submanifolds*. These are submanifolds of the manifold M such

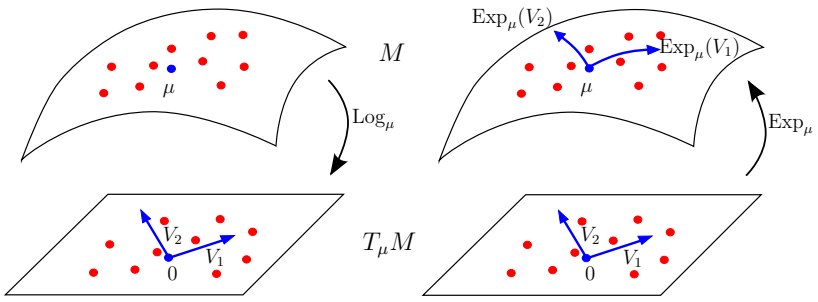

Figure 2: Left: The training data (red) on the shape manifold M and their logarithms on $T_\mu M$. On $T_\mu M$ the principal components V_1 and V_2 of the projected training data are computed (blue). Right: The approximated principal geodesics are obtained by mapping V_1 and V_2 back to M by the exponential map.

that geodesics in the submanifolds are also geodesic in M. In [10] the mean and principal geodesic submanifolds are defined intrinsically. Here, we proceed directly with the definition of the *approximated PGA*:

DEFINITION 3.1. Assume M and data points $p_1, \ldots, p_S \in M$ as above and $p \in M$ (sufficiently close to the data points). We define the *approximated mean* μ of $p_1, \ldots, p_S$ as

$$\mu := \operatorname{Exp}_p \left(\frac{1}{S} \sum_{s=1}^{S} \operatorname{Log}_p(p_s) \right). \tag{1}$$

Let $E_1, \ldots, E_N$ be an orthonormal basis of $T_\mu M$, $\operatorname{Log}_\mu(p_s) = w_s^i E_i$, $1 \le s \le S$, and

$$\Sigma = \frac{1}{S} \sum_{s=1}^{S} w_s w_s^t \in S(N). \tag{2}$$

We call (μ, Σ) the *approximated Principal Geodesic Analysis (approximated PGA)* of the data $p_1, \ldots, p_S$ with respect to the basis $E_1, \ldots, E_N$.

In other words, the approximated PGA is obtained by projecting the data points onto the tangent space using the logarithmic map and then performing a PCA on the tangent space. An illustrative interpretation of this procedure is given in Figure 2.

4 SEGMENTATION FUNCTIONAL AND REGULARIZATION

4.1 The Mahalanobis distance on M

For a given a vector $\mu \in \mathbb{R}^N$ and a symmetric and positive definite matrix $\Sigma \in S(N)$ the *Mahalanobis distance* $d_\Sigma(x, y)$ of two points $x, y \in \mathbb{R}^N$ is defined by $d_\Sigma^2(x, y) = (x - y)^t \Sigma^{-1} (x - y)$. Usually μ and Σ correspond to the mean and the covariance of normally distributed data on $\mathbb{R}^N$.

Our goal is the extension of the above definition to Riemannian manifolds. We assume a fixed $\mu \in M$, a fixed orthonormal basis $E_1, \ldots, E_N$ of $T_\mu M$ with respect to the metric $\langle \cdot, \cdot \rangle_\mu$ and a symmetric, positive definite matrix $\Sigma \in S(N)$. This matrix defines an inner product $\langle \cdot, \cdot \rangle_\Sigma$ on $T_\mu M$ by $\langle v^i E_i, w^i E_i \rangle_\Sigma = v^t \Sigma^{-1} w$ for two tangent vectors $v^i E_i$ and $w^i E_i$ in $T_\mu M$.

Denote the set of all points in M which can be reached by a uniquely determined geodesic starting in μ as $\mathcal{U}$. As in [11] we transport the frame $E_1, \ldots, E_N$ to any

point of $p \in \mathcal{U}$ along the corresponding geodesic. Thus, we have frames $E_n(p)$, $1 \leq n \leq N$, $p \in \mathcal{U}$. Then we define the *Mahalanobis metric* $\langle \cdot, \cdot \rangle_{p,\mu,\Sigma}$ with respect to μ and Σ by

$$\left\langle v^i E_i(p), w^i(p) E_i(p) \right\rangle_{p,\mu,\Sigma} = v^t \Sigma^{-1} w \,, \tag{3}$$

for two tangent vectors $v^i E_i(p)$ and $w^i E_i(p)$ in $T_p M$.

The *Mahalanobis distance* $d_{M,\mu,\Sigma}$ from p to q on $\mathcal{U}$ with respect to μ and Σ is given by

$$d_{M,\mu,\Sigma}(p,q) = \inf_{\substack{\gamma:[0,1]\to\mathcal{U} \\ \gamma(0)=p \\ \gamma(1)=q}} \int_0^1 \langle \dot{\gamma}, \dot{\gamma} \rangle_{p,\mu,\Sigma}^{\frac{1}{2}} \, dt \,, \tag{4}$$

where γ is a piecewise differentiable curve. Note that the Mahalanobis distance on manifolds depends not only on Σ but also on the mean μ. This is not the case in the vector space setting.

4.2 The Regularization Functional

For an edge based segmentation of a 2D image $u : \mathbb{R}^2 \supseteq \Omega \to \mathbb{R}$ we consider the following segmentation energy

$$I_\alpha(p) = -\int_\gamma \left| \nabla u\big(\psi(p)(\tau)\big) \right| d\tau + \alpha d^2_{M,\mu,\Sigma}(\mu, p) \,, \tag{5}$$

which maps a shape parameter p on the sum of the gradient of u along the shape boundary (Snakes energy, [12]) and the Mahalanobis distance from p to μ. Here $\alpha > 0$ is the *regularization parameter*. The parameters μ and Σ are determined by performing an approximated PGA on manually segmented training data as described in the previous section. To detect the shape $\psi(p)$ on u we minimize (5) over $\mathcal{U}$. In case $\mathcal{U} = M$ the existence of a minimizer of I_α has been proven [11].

5 IMPLEMENTATION AND RESULTS

To detect multiple shapes (of the same type) in image data we generalize (5) to

$$(p_1, \ldots, p_R) \mapsto \sum_{r=1}^{R} I_\alpha(p_r) \,. \tag{6}$$

for a fixed number R of shapes. The idea is to minimize (6) subject to the constraint that the shapes $\psi(p_r)$, $1 \leq r \leq R$, do not overlap each other. We applied this idea to the detection of cells in microscope images as in Figure 3. The approximated PGA for the regularization term in I_α was computed from the 18 training shapes in the upper left image. For the minimization we used the following heuristic algorithm:

1. Initialize a vector $c_1 = \ldots = c_R = C$ for some $C > 0$ and a vector of shape parameters $(p_1, \ldots, p_R) \in M^R$.

2. Choose a random shape $p' \in B_C := \{p \in M : d_{M,\mu,\Sigma}(\mu, p) \leq C\}$. If $I_\alpha(p') < c_r$ for an index $1 \leq r \leq R$ and $\psi(p')$ does not overlap with any of the shapes $\psi(p_1), \ldots, \psi(p_R)$, replace p_r by p' and set $c_r = I_\alpha(p')$. If it overlaps with the shapes $\psi(p_{r_1}), \ldots, \psi(p_{r_k})$ and $I_\alpha(p') < \min(c_{r_1}, \ldots c_{r_k})$, then replace p_{r_1} by p' and set $c_{r_1} = I_\alpha(p')$ and $c_{r_2} = \ldots = c_{r_k} = C$, respectively. Repeat this step.

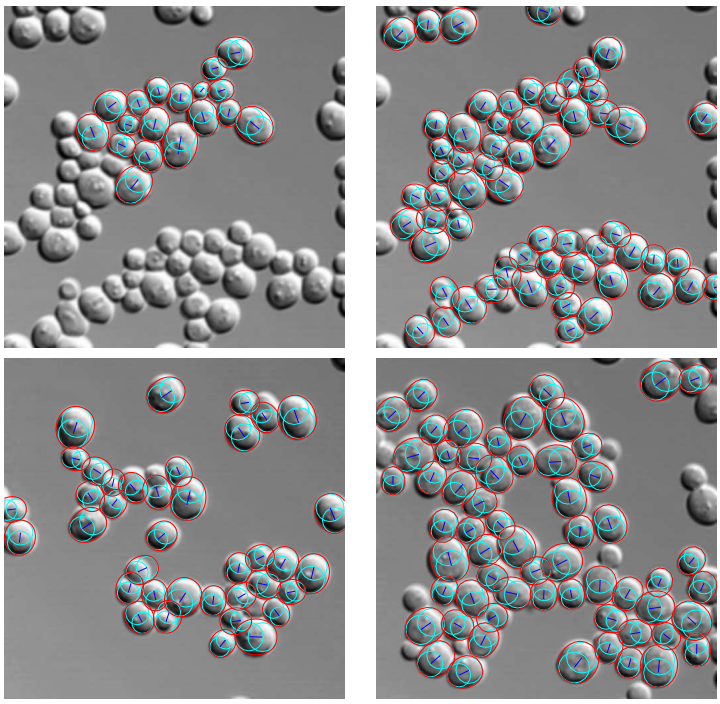

Figure 3: Upper left image: Expert segmentation of 18 cells. Upper right and lower row: Automatic detection of cells.

In simple words, we generate random shape parameters and try to improve the current segmentation by replacing one of the shapes defined by $(p_1, \ldots, p_R)$ by the newly generated parameters. This gradually improves the segmentation of the result. This algorithm is far from being efficient and in fact does not necessarily lead to the best result, but it is able to demonstrate two important issues:

1. We do not have to evaluate the gradient of I_α in this example. Moreover the danger of being trapped at local minima is much smaller than with gradient descent techniques. This means that we are able to detect different cells even if they are clustered as in our examples. An active contour algorithm [6] can not handle this situation, since features *inside* the clusters have to be considered for a correct segmentation.

2. The first property is a characteristic of Monte Carlo optimization techniques in general. However, it is impossible to randomly sample the entire shape space M. One has to agree on some subset of "probable" or "meaningful" shapes. In our case this selection is canonically given by choosing shapes close to the mean shape and varying them according to the training data. In other words, by choosing shapes in B_C we generate only shapes, which we expect to actually appear in the image data, as candidates for a correct segmentation.

Acknowledgments: This work has been supported by the Austrian Science Foundation (FWF) Projects FSP9202-N12, FSP9203-N12 and FSP9207-N12. We thank Heimo Wolinski, IMB-Graz, Karl-Franzens-Universität, Graz, Austria, and Bettina Heise, FLLL, Linz-Hagenberg, Austria, for the microscope images.

REFERENCES

[1] Daniel Cremers, Florian Tischhäuser, Joachim Weickert, and Christoph Schnörr. Diffusion snakes: Introducing statistical shape knowledge into the mumford-shah functional. *Int. J. Comp. Vis.*, 50(3):295–313, 2002.

[2] Yunmei Chen, Hemant D. Tagare, Sheshadri Thiruvenkadam, Feng Huang, David Wilson, Kaundinya S. Gopinath, Richard W. Briggs, and Edward A. Geiser. Using prior shapes in geometric active contours in a variational framework. *Int. J. Comp. Vis.*, 50(3):315–328, 2002.

[3] Micheal E. Leventon, W. Eric L. Grimson, and Olivier Faugeras. Statistical shape influence in geodesic active contours. In *IEEE Conference on Computer Vision and Pattern Recognition*, volume 1, pages 316–323, June 2001.

[4] Mikael Rousson and Nikos Paragios. Shape priors for level set representations. In Anders Heyden, Gunnar Sparr, Mads Nielsen, and Peter Johansen, editors, *Computer Vision - ECCV 2002 : 7th European Conference on Computer Vision, Copenhagen, Denmark, May 28-31, 2002. Proceedings, Part II*, volume 2351 of *Lect. Notes Comp. Sci.*, pages 78–92. Springer, 2002.

[5] Andy Tsai, Anthony Yezzi, Clare Tempany, Dewey Tucker, Ayres Fan, W. Eric L. Grimson, and Alan Willsky. A shape-based approach to the segmentation of medical imagery using level sets. *IEEE Trans. Med. Imag.*, 22(2):137–154, 2003.

[6] Vicent Caselles, Ron Kimmel, and Guillermo Sapiro. Geodesic active contours. *Int. J. Comp. Vis.*, 22(1):61–79, 1997.

[7] David Mumford and Jayant Shah. Optimal approximations by piecewise smooth functions and associated variational problems. *Comm. Pur. Appl. Math.*, 42(4):577–684, 1989.

[8] Sarang Joshi, Stephen Pizer, P. Thomas Fletcher, Paul Yushkevich, Andrew Thall, and J. S. Marron. Multiscale deformable model segmentation and statistical shape analysis using medial descriptions. *IEEE Trans. Med. Imag.*, 21(5):538–550, 2002.

[9] William M. Boothby. *An Introduction to Differentiable Manifolds and Riemannian Geometry*, volume 63 of *Pure and Applied Mathematics*. Academic Press, New York, 1975.

[10] P. Thomas Fletcher, Conglin Lu, and Sarang Joshi. Statistics of shape via principal geodesic analysis on lie groups. In *Computer Vision and Pattern Recognition, 2003. Proceedings. 2003 IEEE Computer Society Conference on*, volume 1, pages 95–101, 2003.

[11] Matthias Fuchs and Otmar Scherzer. Regularized reconstruction of shapes with statistical a priori knowledge. Technical Report 51, FSP 092, May 2007.

[12] Micheal Kass, Andrew Witkin, and Demetri Terzopoulos. Snakes active contour models. *Int. J. Comp. Vis.*, 1(4):321–331, 1988.